EUROPEAN TRANSACTIONS ON ELECTRICAL POWER
Euro. Trans. Electr. Power 2005; **15**:203–216
Published online in Wiley InterScience (www.interscience.wiley.com). DOI: 10.1002/etep.52

A spectral method for on-line computation of the harmonics of symmetrical components in induction machines

T. Assaf, H. Henao*,† and G. A. Capolino

Department of Electrical Engineering—CREA, University of Picardie—Jules Verne, 33 rue Saint Leu, 80039 Amiens Cedex 1, France

SUMMARY

This paper describes a procedure for the on-line computation of the harmonics of symmetrical components for voltages, currents and impedances in working induction machines. The algorithm used to compute these components is based on the discrete Fourier transform (DFT) of complex sequences. An experimental test-bed with a 0.12 kW star-connected induction motor has been used to test the procedure. The stability of the numerical results is verified to show the performance of the proposed method. Copyright © 2005 John Wiley & Sons, Ltd.

KEY WORDS: on-line computation; induction machines; harmonics; symmetrical components; discrete Fourier transform

1. INTRODUCTION

In the industrial world, the profits of productivity represent a daily preoccupation for the leaders of companies. The diagnosis of failures in industrial systems, if it is carried out with effectiveness or if it makes early detection of degradation possible, represents one of the means to contribute to improving productivity. Failures causing a partial or total stoppage of equipment can represent considerable economic losses, even before taking into account the impact on the environment and danger to people. The renewed interest expressed by the various industrial sectors and the research world shows that this field develops constantly. In fact, lots of instruments have been tested but, in the literature, there are insufficient theoretical arguments to justify its operating principle. The fault classification for induction machines has been presented already in several publications [1–7]. If interest is concentrated on electrical faults, it has to be related to the stator windings and to the rotor electrical configurations, considering only the squirrel cage structure that represents more than 99% of the induction machines manufactured in the last ten years. Then, it is interesting to note that each electrical fault can have on influence on both electrical and mechanical variables that can be measured around the induction machine itself [1].

Stator faults are usually related to insulation failure and they are generally known as phase-to-phase or phase-to-neutral faults. The primary causes of stator failure insulation are [2]: high stator core or

*Correspondence to: H. Henao, Department of Electrical Engineering—CREA, University of Picardie—Jules Verne, 33 rue Saint Leu, 80039 Amiens Cedex 1, France.
†E-mail: Humberto.Henao@u-picardie.fr

winding temperatures, short-circuit or starting stresses, electrical discharges, leakage in cooling systems, and contamination due to oil, moisture or dirt. Rotor faults are related to rotor bar and end-ring breakage. They can be caused by thermal stresses due to thermal overload and imbalance, hot spots or excessive losses, magnetic stresses caused by electromagnetic forces, unbalanced magnetic pull, electromagnetic noise and vibration or bearing failure, etc.

The usual method for both stator and rotor fault detection is based on the motor current signature analysis (MCSA) [3–6]. For this purpose, the information given by stator current sensors is necessary to analyse the machine behaviour. With this approach, the lower and upper twice slip frequency sidebands around the fundamental frequency given by $(1 \pm 2.s)f_1$ are used when a rotor asymmetry occurs. This phenomenon can be explained as the result of a backward rotating field induced by the rotor fault. These classical frequency sidebands due to the machine space harmonics are not the only effects due to the broken rotor bars. Other frequencies in the stator current due to the space harmonics and also to the power supply harmonics are induced. In the literature, these contributions are insufficiently analysed and explained to improve the decision process on rotor and stator asymmetries and their respective severities.

Since the electrical machines are part of power system networks, the detection of their electrical faults are necessarily related to the network faults [7]. In this way, the objective of this paper is to analyse the behaviour of the induction machine from the point of view of the network that feeds it. It is a different way to analyse and to detect the electrical fault by discrimination of power supply and power load independent behaviours. In this way, MCSA is not enough to decide and the voltage measurement is mandatory. The study of the faults influence on the power network for a safe electrical machine and the reverse effect is of great importance for instrument design. In fact, a power network is neither balanced nor free of harmonics and this leads to the fact that modern signal processing techniques are key points to perform the measurements for fault monitoring. The usage of modern signal processing techniques in power systems is not new and many papers have been written in this domain [8–10] contributing to the development of specific digital instruments and permitting the real shape of the waveforms detected to be taken into account. On the other hand, two new textbooks give the most interesting algorithms to perform digital signal processing and to implement them on standard and low-cost hardware [11,12].

Traditionally, the analysis of an induction machine under unbalanced voltage conditions has been performed using the method of symmetrical components applied to the main signal harmonic. Information on the symmetrical components can be used to prevent machine damage or the degradation of the torque-speed machine characteristics. The difficulty of measuring the phase angle between the system phasors has led to the development of complex algorithms [13–17] limiting the analysis to the fundamental components of line currents and line-to-line voltages and filtering many important bits of information as harmonic components.

The description of the computation method for the symmetrical components of an induction machine based on the discrete Fourier transform (DFT) has been presented already [17–19]. The new contribution is based on the application of this technique to the computation of all the harmonics contained in the power source and the load. In this sense, the information given by time harmonics in the power supply can be used to analyse the power source and the machine asymmetries starting from current, voltage, impedance symmetrical components and completing the classical observation obtained by the study of the main harmonic component.

The first part of this paper is related to the theory of the symmetrical components in the presence of harmonics. The second part describes a spectral digital method for the computation of the harmonics of symmetrical components for voltages, currents and impedances of the induction motor under test.

The proposed method is tested experimentally to measure the harmonics of symmetrical components of a working induction motor for periodic or continuous monitoring. The stability of the results is tested for a wide interval of voltage source dissymmetry levels and for different load levels. This method will be used to monitor power quality and to detect electrical faults from the power source and load with the same measurements.

2. SYMMETRICAL COMPONENTS THEORY

Considering the phasor vectors of line-to-neutral voltages $[\underline{\boldsymbol{V}}_a\underline{\boldsymbol{V}}_b\underline{\boldsymbol{V}}_c]^{\mathrm{T}}$ and line currents $[\underline{\boldsymbol{I}}_a\underline{\boldsymbol{I}}_b\underline{\boldsymbol{I}}_c]^{\mathrm{T}}$ associated with the same load, the symmetrical components of voltages and currents are defined by the vectors $[\underline{\boldsymbol{V}}_1\underline{\boldsymbol{V}}_2\underline{\boldsymbol{V}}_0]^{\mathrm{T}}$ and $[\underline{\boldsymbol{I}}_1\underline{\boldsymbol{I}}_2\underline{\boldsymbol{I}}_0]^{\mathrm{T}}$, respectively. The subscripts 1-2-0 refer to the positive, negative and zero sequence, respectively. In the case of an unbalanced induction machine, each sequence sees a different impedance from all others without any interaction between them. This means that the transformation from *a-b-c* co-ordinates to 1-2-0 co-ordinates decouples the machine operation completely from the point of view of voltages and currents at the stator side. The impedances seen are usually noted as $\underline{\boldsymbol{Z}}_1$, $\underline{\boldsymbol{Z}}_2$ and $\underline{\boldsymbol{Z}}_0$ for the positive, negative and zero sequences, respectively. The behaviour of an induction motor connected to an unbalanced power system can be analysed by studying its equivalent positive and negative circuits as usually presented in the literature (Figure 1).

The general expression of the induction machine slip as a function of the rank of time harmonics h is given by Equation (1):

$$s_h = \frac{h\omega - p\Omega}{h\omega} \tag{1}$$

where p is the number of pole pairs, Ω is the rotor speed and ω is the angular frequency of power supply.

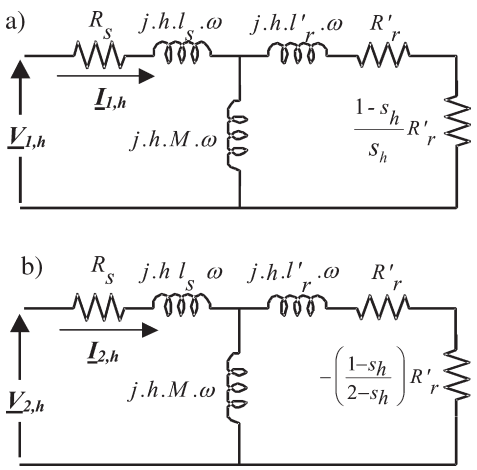

Figure 1. Equivalent circuits for three-phase induction motor: (a) Positive sequence; (b) negative sequence.

The complex symmetrical components of voltages and currents are related by the following matrix equation:

$$\begin{bmatrix} \underline{\boldsymbol{V}}_{1,h} \\ \underline{\boldsymbol{V}}_{2,h} \\ \underline{\boldsymbol{V}}_{0,h} \end{bmatrix} = \begin{bmatrix} \underline{\boldsymbol{Z}}_{1,h} & 0 & 0 \\ 0 & \underline{\boldsymbol{Z}}_{2,h} & 0 \\ 0 & 0 & \underline{\boldsymbol{Z}}_{0,h} \end{bmatrix} \cdot \begin{bmatrix} \underline{\boldsymbol{I}}_{1,h} \\ \underline{\boldsymbol{I}}_{2,h} \\ \underline{\boldsymbol{I}}_{0,h} \end{bmatrix} \tag{2}$$

Industrial power distribution systems with non-linear loads usually contain a great number of harmonic components which are largely produced by the static power converters. In the strictly balanced six-pulse based converter, only $6j \pm 1$ (with $j = 0, 1, 2, 3, \ldots$) harmonic components are presented by Fourier analysis. The power source harmonics are principally low-frequency harmonics such as 1st, 5th, 7th, 11th, 13th, ... The effect of these harmonics in the induction machine air-gap is a magnetomotive force that turns at speeds of ω, -5ω, 7ω, -11ω, $13\omega, \ldots$, for each harmonic component, respectively. So, the positive components of harmonics 5th, 11th, ..., of both voltage and current can be located in the reverse direction with respect to the positive component of the 1st harmonic ω. The corresponding negative components are then located in the same direction of the 1st harmonic ω. The direct components of harmonics 7th, 13th, ..., of both voltage and current can be located in the same direction as for the positive component of the 1st harmonic ω and the negative one in the reverse direction. Then, the expression of the induction machine slip given by Equation (1) must be affected by the harmonic rotational sense.

Since induction motors are usually wound either for Δ or ungrounded Y connection, the zero sequence currents in the motor are always zero and there is no need for a zero sequence impedance computation. Positive and negative harmonic sequence impedances can be expressed in the complex form by:

$$\underline{\boldsymbol{Z}}_{1,h} = \frac{\underline{\boldsymbol{V}}_{1,h}}{\underline{\boldsymbol{I}}_{1,h}} \tag{3}$$

$$\underline{\boldsymbol{Z}}_{2,h} = \frac{\underline{\boldsymbol{V}}_{2,h}}{\underline{\boldsymbol{I}}_{2,h}} \tag{4}$$

with $h = 1, 5, 7, 11, 13, \ldots$.

In order to determine the different harmonic components of both voltage and current with non-sinusoidal conditions, a signal processing has to be carefully designed to match the signal characteristics with respect to the fundamental harmonic. In the steady-state conditions, it is suspected that the voltage $v(t)$ and the current $i(t)$ are periodic over the interval T_1 given by the power system frequency f_1 ($T_1 = 1/f_1$). Although not purely sinusoidal, they are assumed to contain a finite number $(M-1)$ of harmonics. Then, the sampling period may be chosen as:

$$T_s = \frac{T_1}{2(M-1)} \tag{5}$$

3. DFT FOR HARMONICS OF SYMMETRICAL COMPONENTS COMPUTATION

The DFT can be carried out with either real or complex sequences. The N samples time-domain signal $X_s[n]$ with the DFT given by $S[k]$ is decomposed into a set of $N-1$ cosine waves and $N-1$ sine waves with frequencies given by the index k. The magnitudes of the cosine waves are contained in the real part of the sequence $\mathrm{Re}\{S[k]\}$ while the magnitudes of the sine waves are contained in the imaginary part $\mathrm{Im}\{S[k]\}$. Sine and cosine waves can be described as having a positive frequency or a negative frequency. Since in a real sequence the two views are identical, the Fourier transform represents negative frequencies with positive values in the same spectrum with only positive frequencies.

In the complex Fourier transform, both $X_s[n]$ and $S[k]$ are arrays of complex numbers. The complex Fourier transform includes both positive and negative frequencies which means that $k=0,\ldots,N-1$ where N is the total number of samples. The reduced frequencies between 0 and $(N/2)-1$ are positive, while the reduced frequencies between $(N/2)+1$ and $N-1$ are negative, where $k=N/2$ corresponds with the Nyquist frequency and $k=0$ corresponds with the DC component.

With a three-phase set of sampled voltages $v_a[n]$, $v_b[n]$, $v_c[n]$ and a three-phase set of sampled currents $i_a[n]$, $i_b[n]$, $i_c[n]$, each one of the signals is obtained by using digital processing. The associated sampled complex voltage vector $\underline{\boldsymbol{V}}[n]$ and current vector $\underline{\boldsymbol{I}}[n]$ are given by (bold for vectors):

$$\begin{aligned}\underline{\boldsymbol{V}}[n] &= \frac{2}{3}\left[v_a[n]+v_b[n]\mathrm{e}^{j\frac{2}{3}\pi}+v_c[n]\mathrm{e}^{-j\frac{2}{3}\pi}\right]\\ \underline{\boldsymbol{I}}[n] &= \frac{2}{3}\left[i_a[n]+\mathrm{i}_b[n]\mathrm{e}^{j\frac{2\pi}{3}}+i_c[n]\mathrm{e}^{-j\frac{2\pi}{3}}\right]\end{aligned} \tag{6}$$

The constant coefficient 2/3 is chosen to make the vector magnitudes $|\underline{\boldsymbol{V}}[n]|$ and $|\underline{\boldsymbol{I}}[n]|$ equal to the peakvalue of the phase voltage and the line current, respectively, for the symmetrical sinusoidal case.

In fact, the voltage and current harmonic sequence components can be obtained directly by applying DFT to complex sequences $\underline{\boldsymbol{V}}[n]$ and $\underline{\boldsymbol{I}}[n]$, respectively (Figure 2). The finite complex

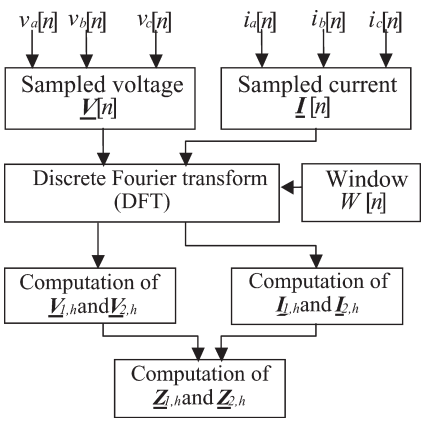

Figure 2. Positive and negative sequence impedances computation using complex DFT.

sequences $\underline{\boldsymbol{V}}_w[n]$ and $\underline{\boldsymbol{I}}_w[n]$, that are digitally windowed values of $\underline{\boldsymbol{V}}[n]$ and $\underline{\boldsymbol{I}}[n]$, give the following frequency spectrum:

$$\begin{aligned}\underline{\boldsymbol{V}}_w[k] &= \frac{1}{N}\sum_{k=0}^{N-1}\boldsymbol{V}_w[n]\mathrm{e}^{-j\frac{2pk}{N}n}\\ \underline{\boldsymbol{I}}_w[k] &= \frac{1}{N}\sum_{k=0}^{N-1}\boldsymbol{I}_w[n]\mathrm{e}^{-j\frac{2pk}{N}n}\end{aligned} \tag{7}$$

with a spectrum frequency resolution given by:

$$\Delta f = \frac{1}{T_S N} \tag{8}$$

Voltage and current positive harmonic sequences $\underline{\boldsymbol{V}}_{1,1}, \underline{\boldsymbol{I}}_{1,1}, \underline{\boldsymbol{V}}_{1,7}, \underline{\boldsymbol{I}}_{1,7}, \underline{\boldsymbol{V}}_{1,13}, \underline{\boldsymbol{I}}_{1,13}, \ldots$ are given by the corresponding positive frequencies (f_1, $7f_1$, $13f_1, \ldots$) and the negative ones by the corresponding negative frequencies ($-f_1$, $-7f_1$, $-13f_1, \ldots$) as follows (Figure 3):

$$\begin{aligned}\underline{\boldsymbol{V}}_{1,1} &= \underline{\boldsymbol{V}}_w\left[k_{f1}\right] & \underline{\boldsymbol{I}}_{1,1} &= \underline{\boldsymbol{I}}_w\left[k_{f1}\right]\\ \underline{\boldsymbol{V}}_{1,7} &= \underline{\boldsymbol{V}}_w\left[7k_{f1}\right] & \underline{\boldsymbol{I}}_{1,7} &= \underline{\boldsymbol{I}}_w\left[7k_{f1}\right]\\ \underline{\boldsymbol{V}}_{1,13} &= \underline{\boldsymbol{V}}_w\left[13k_{f1}\right] & \underline{\boldsymbol{I}}_{1,13} &= \underline{\boldsymbol{I}}_w\left[13k_{f1}\right]\\ &\vdots & &\vdots\\ \underline{\boldsymbol{V}}_{2,1} &= \underline{\boldsymbol{V}}_w\left[N-k_{f1}\right] & \underline{\boldsymbol{I}}_{2,1} &= \underline{\boldsymbol{I}}_w\left[N-k_{f1}\right]\\ \underline{\boldsymbol{V}}_{2,7} &= \underline{\boldsymbol{V}}_w\left[N-7k_{f1}\right] & \underline{\boldsymbol{I}}_{2,7} &= \underline{\boldsymbol{I}}_w\left[N-7k_{f1}\right]\\ \underline{\boldsymbol{V}}_{2,13} &= \underline{\boldsymbol{V}}_w\left[N-13k_{f1}\right] & \underline{\boldsymbol{I}}_{2,13} &= \underline{\boldsymbol{I}}_w\left[N-13k_{f1}\right]\\ &\vdots & &\vdots\end{aligned} \tag{9}$$

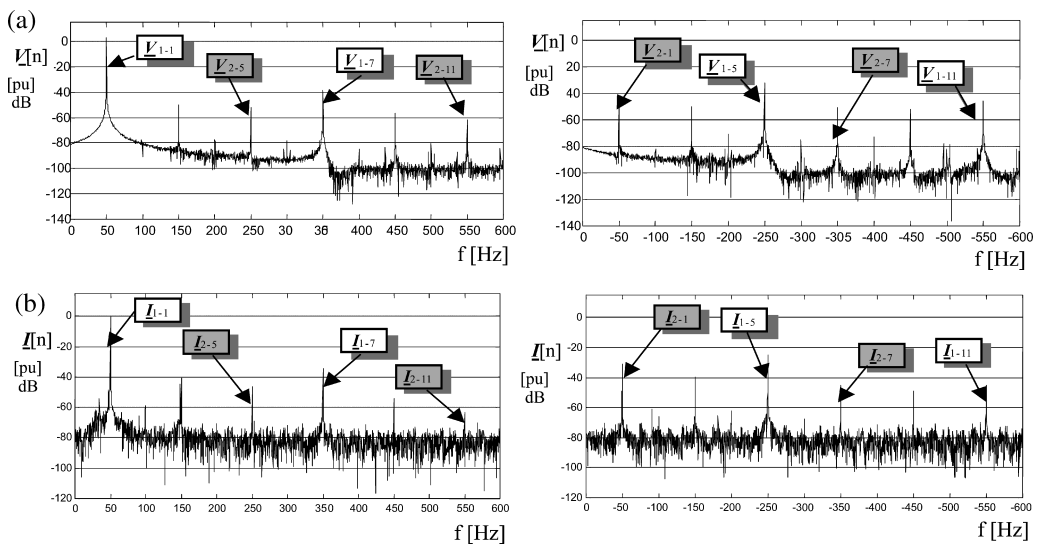

Figure 3. Localization of the harmonics of both positive and negative components of voltages and currents into the spectrum of (a) $\underline{\boldsymbol{V}}[n]$, and (b) $\underline{\boldsymbol{I}}[n]$.

with

$$k_{f1} = \frac{N}{2(M-1)}$$

Voltage and current positive harmonic sequences $\underline{\boldsymbol{V}}_{1,5}$, $\underline{\boldsymbol{I}}_{1,5}$, $\underline{\boldsymbol{V}}_{1,11}$, $\underline{\boldsymbol{I}}_{1,11}, \ldots$. are given by the corresponding negative frequencies ($-5f_1$, $-11f_1, \ldots$.) and the negative ones by the corresponding positive frequencies ($5f_1$, $11f_1, \ldots$.) as follows:

$$\begin{array}{ll}
\underline{\boldsymbol{V}}_{1,5} = \underline{\boldsymbol{V}}_w\left[N - 5k_{f1}\right] & \underline{\boldsymbol{I}}_{1,5} = \underline{\boldsymbol{I}}_w\left[N - 5k_{f1}\right] \\
\underline{\boldsymbol{V}}_{1,11} = \underline{\boldsymbol{V}}_w\left[N - 11k_{f1}\right] & \underline{\boldsymbol{I}}_{1,11} = \underline{\boldsymbol{I}}_w\left[N - 11k_{f1}\right] \\
\vdots & \vdots \\
\underline{\boldsymbol{V}}_{2,5} = \underline{\boldsymbol{V}}_w\left[5k_{f1}\right] & \underline{\boldsymbol{I}}_{2,5} = \underline{\boldsymbol{I}}_w\left[5k_{f1}\right] \\
\underline{\boldsymbol{V}}_{2,11} = \underline{\boldsymbol{V}}_w\left[11k_{f1}\right] & \underline{\boldsymbol{I}}_{2,11} = \underline{\boldsymbol{I}}_w\left[11k_{f1}\right] \\
\vdots & \vdots
\end{array} \tag{10}$$

Then, with the values obtained in Equations (9) and (10), positive and negative harmonic sequence impedances can be computed using Equations (3) and (4).

The results presented in Figure 3 correspond to a star-connected induction motor. In this case, the present components associated to rank multiple of 3 are due to the imbalance in the current sensor transfer ratio and the non-simultaneous sampling of the data acquisition system.

The impedance measurement can be influenced positively by the space harmonics already present in the induction machine only under certain conditions:

- when a rotor asymmetry is detected
- when the rotor slip is too low (no-load)
- when the frequency resolution is too low

In fact, these conditions do not allow discrimination of the concerned source harmonic and the nearest frequency component associated to the space harmonic. For a significant rotor slip under the same conditions of rotor asymmetry, the effect of space harmonics in the stator spectrum is the presence of slip frequency sidebands around the fundamental and the power source harmonics.

The analysis of Equation (4) for the fundamental harmonic has shown that a healthy induction machine presents a nearly constant negative impedance for both theoretical and analytical points of view. However, for different levels of failure applied to the stator windings (inter-turn short-circuits from 1% to 17% of the total phase winding turns), the evolution of the negative impedance shows a near-linear reduction in its per unit module starting from the initial value in the healthy conditions. It is important to mention that the negative impedance is not only related to stator or rotor faults. Even for a healthy machine, the negative impedance is present for the fundamental and the other harmonics. Then, the negative impedance harmonics obtained are the base values which have to be taken into account to reflect the manufacturing imperfections. This is the reason why both the voltage and current spectrum are computed, the voltage being related to the power source and the current to the electrical machine. In fact, there is a small interaction between both since the voltage measurement is performed at the machine terminals and is influenced by the line impedance which is usually unknown.

4. EXPERIMENTAL RESULTS

4.1. Test-bed description

To test the diagnostic techniques on three-phase induction machines, our lab has designed a number of platforms. Each platform is equipped with dedicated sensors to analyse different aspects of the machine operation. The facilities used to perform tests with classical electrical sensors (voltage, current) are limited to a power of 5 kW.

A 0.12 kW induction machine has been used to implement this method but a more powerful machine can be used too without loss of generality. In fact, it is well known that the secondary effects due to the skin effect, iron loss and stator resistance decreases in significance with respect to the increase of the machine power. The interest in the proposed approach is that the induction machine can be analysed by its equivalent positive and negative circuits for all power ranges and with *per unit* (pu) representation.

A specific experimental set-up has been designed in order to test the algorithm (Figure 4). It is based on a three-phase voltage source that facilitates the simulation of a set of unbalanced voltages. A 0.12 kW, 50 Hz, 220 V/380 V, 2-pole three-phase induction motor is used, as a machine under test (MUT), to observe the behaviour of the symmetrical components (voltage, current and impedance) under the effect of a voltage source dissymmetry. A magnetic brake, which can be controlled by means of a control unit, has been used to simulate the shaft load.

The induction machine voltages and currents are measured by means of three voltage sensors and three current sensors connected to the terminals. The six signals are used as inputs of the signal

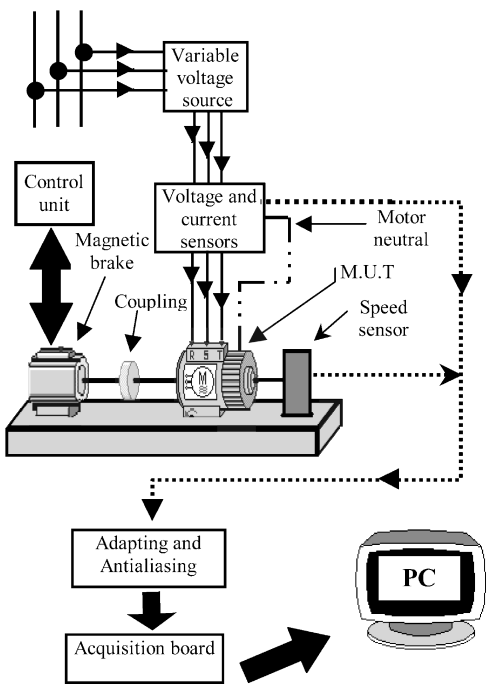

Figure 4. Configuration of the test-bed.

conditioning and the data acquisition board integrated into a personal computer (PC). The current probes are realized with Rogowski coils with a typical frequency bandwidth of 50 kHz. The voltage sensors are special transformers with large frequency bandwidth of 5 kHz which allows the galvanic insulation and the observation on the frequency spectrum of the low frequencies associated with the considered model of induction machine. Sensors with larger frequency bandwidth are not necessary since they need to be concerned with induction machine models at high frequency with capacitive effects. The algorithm for the symmetrical components' evaluation and all the digital operations have been implemented by using the MATLAB^{TM} environment.

4.2. Computation of symmetrical components and their harmonics

The first stage in the experimental study consists of the analysis of the time-domain evolution for the stator voltages and currents of the induction machine in test with four levels of unbalanced voltage source that affects only one-phase voltage magnitude with 0%, −5%, −10% and −20% of the rated phase voltage. This voltage imbalance can be expressed as:

$$\gamma_x[\boldsymbol{pu}] = \frac{\boldsymbol{v}_{x\text{-rms}}}{\boldsymbol{v}_{n\text{-rms}}} - 1 \tag{11}$$

Thus, each one of the previous cases has been performed with the induction machine operating at five levels of mechanical load: from 0 to 100% of the rated value, in steps of 25%. For each case, the stator voltages and currents have been collected within a time period large enough (3.5 s, i.e. 175 periods) to perform averaging. For these cases of power supply imbalance, only the negative sequences are analysed.

The modulus of the fundamentals negative components ($\underline{\boldsymbol{V}}_{2,1}$, $\underline{\boldsymbol{I}}_{2,1}$ and $\underline{\boldsymbol{Z}}_{2,1}$) of the induction machine in test and their harmonics ($\underline{\boldsymbol{V}}_{2,h}$, $\underline{\boldsymbol{I}}_{2,h}$ and $\underline{\boldsymbol{Z}}_{2,h}$) have been computed by the mean of the proposed method. Thus, the experimental results to study the component evolution have been analysed as a function of the induction machine load level and the imbalance level applied to one phase of the power supply. This analysis has been performed with three-dimensional representation pictures showing the lines of constant value (height) for the module of the analysed variables.

The effect of voltage source dissymmetry on the negative sequence of voltage and current of both the first harmonic (Figure 5) and the fifth one (Figure 6) is clearly indicated looking to the evolution of its magnitude with respect to the power supply dissymmetry level. The equivalent parameters are given in p.u. with reference to the rated values of both stator voltage and line current. The 3D representations show clearly that the numerical results are quite stable since the surfaces have no singularities.

However, $\underline{\boldsymbol{Z}}_{2,5}$, $\underline{\boldsymbol{V}}_{2,5}$, $\underline{\boldsymbol{I}}_{2,5}$ show a small dispersion which corresponds with small numerical values which are the result of a no-load operation with balanced supply voltages, knowing that in theory the equivalent circuit of negative sequence is not excited. In this case, it is suspected that both natural imbalance of the machine windings are superposed with the small imbalance of the power supply without permitting the two phenomena, to be separated.

It is obvious that the inverse voltage magnitude is directly proportional to the imbalance level as expected. The coefficient of proportionality is corrupted for high-level load torque without large difference. For 20% of voltage imbalance, the magnitude of the voltage $\underline{\boldsymbol{V}}_{2,1}$ reaches a value around 0.08 p.u.

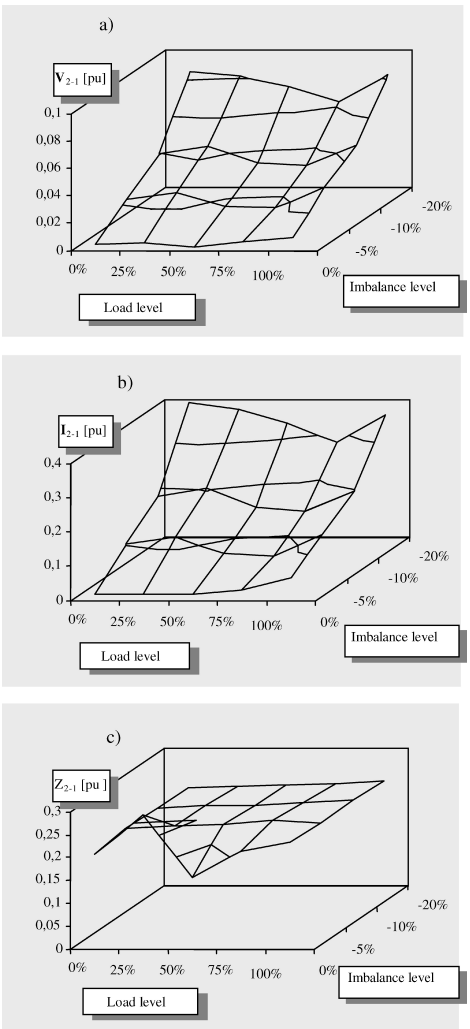

Figure 5. Inverse sequence fundamental components: (a) Voltage; (b) current; and (c) impedance.

The magnitude of the inverse sequence current $\underline{I}_{2,1}$ has the same shape compared to the voltage but the level reached is close to 0.4 p.u. for this induction machine. Then, as expected from the previous operations, the module of the inverse complex impedance $\underline{\boldsymbol{Z}}_{2,1}$ is around 0.2 p.u. except some differences for low levels of both voltage and current.

Concerning the negative components $\underline{\boldsymbol{V}}_{2,5}$, $\underline{\boldsymbol{I}}_{2,5}$ and $\underline{\boldsymbol{Z}}_{2,5}$ of the fifth harmonic (Figure 6), it is clear that they have the same general tendency. Comparing these components with those of the first harmonic, they have less significant values with respect to the level of imbalance. In this case, the machine continues to develop a negative impedance nearly stable (around 0.53 p.u.). However, negative components of voltage and current of harmonics 1st and 5th with respect to those of harmonics 7th and 11th show an insensitivity to the imbalance level and fluctuate in a random way. However, the machine still continues to develop a nearly constant value of negative impedance (Figure 7).

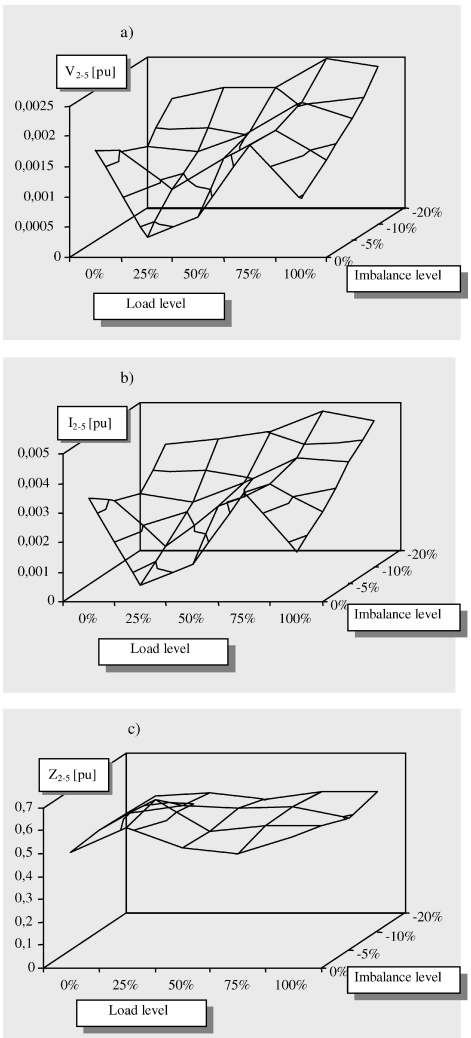

Figure 6. Inverse sequence components for the fifth harmonic: (a) Voltage; (b) current; and (c) impedance.

5. CONCLUSION

A spectral method for on-line computation of the harmonic symmetrical components is used for low-frequency components of voltages, currents and impedances. This method, based on the DFT computation of complex sequences, facilitates the extraction of the information given by power supply harmonics to characterize the induction machine in operation. It can be applied to any three-phase load without loss of generality.

This technique is useful in terms of power quality evaluation and also when the harmonics effects are a key point of interest. The proposed method can be used to detect electrical faults in the machine on the basis of the comparison with respect to the normal operation. The obtained results show the

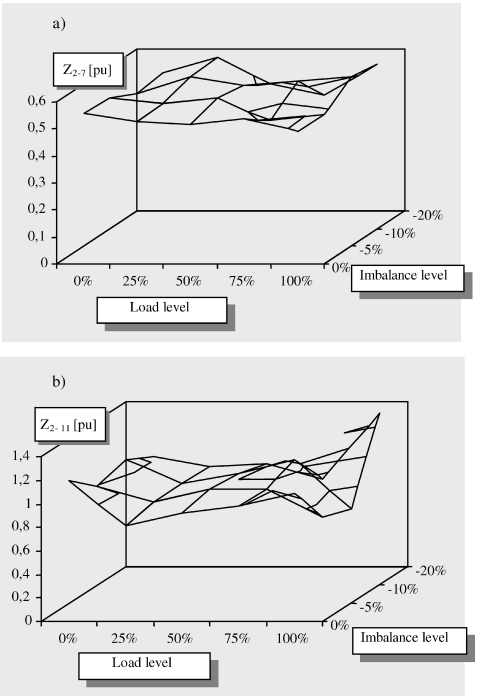

Figure 7. Inverse sequence impedance for harmonics: (a) 7; (b) 11.

efficiency of the method that can be implemented in a simple hardware with low-cost and low-frequency voltage and current sensors. The computer hardware is also simple since it is based on a 16-bit/6 differential analog inputs data acquisition board. Then, the proposed technique opens a new perspective for low-cost digital instrumentation relative to power systems.

6. LIST OF SYMBOLS

$\underline{\boldsymbol{V}}_a$, $\underline{\boldsymbol{V}}_b$, $\underline{\boldsymbol{V}}_c$	line-to-neutral voltage phasors
$v_a[n]$, $v_b[n]$, $v_c[n]$	sampled voltages
$\underline{\boldsymbol{V}}[n]$	sampled complex voltage vector
$\underline{\boldsymbol{V}}_{1,h}$, $\underline{\boldsymbol{V}}_{2,h}$, $\underline{\boldsymbol{V}}_{0,h}$	positive, negative and zero voltage sequence harmonic components
$\underline{\boldsymbol{I}}_a$, $\underline{\boldsymbol{I}}_b$, $\underline{\boldsymbol{I}}_c$	line current phasors
$i_a[n]$, $i_b[n]$, $i_c[n]$	sampled currents
$\underline{\boldsymbol{I}}[n]$	sampled complex current vector
$\underline{\boldsymbol{I}}_{1,h}$, $\underline{\boldsymbol{I}}_{2,h}$, $\underline{\boldsymbol{I}}_{0,h}$	positive, negative and zero current sequence harmonic components
$\underline{\boldsymbol{Z}}_{1,h}$, $\underline{\boldsymbol{Z}}_{2,h}$, $\underline{\boldsymbol{Z}}_{0,h}$	positive, negative and zero impedance sequence harmonic components
T_s	sampling period
f_1	power system frequency
M	number of assumed time harmonics
N	total number of samples

Δf	spectrum frequency resolution
h	rank of time harmonics, $h = 6j \pm 1$ with $j = 0, 1, 2, 3, \ldots$
s_h	motor slip for the h-th harmonic
p	number of pole pairs
Ω	rotor speed
ω	angular frequency of the power supply
γ_x	unbalanced per cent applied to the phase x (a, b, c).
v_x-rms	effective value of line-to-neutral voltage applied to the phase x.
V_n-rms	effective value of line-to-neutral nominal voltage of power supply.

REFERENCES

1. Capolino GA. A comprehensive analysis of the current status in low voltage induction motor diagnosis. Invited paper (plenary session), *Proceedings of the International Conference on Electrical Machines (ICEM'00)*, Vol. 2, Espoo, Finland, August 2000; pp 595–602.
2. Penman J, Sedding HG, Lloyd BA, Fink WT. Detection and location of inter-turn short circuits in the stator windings of operating motors. *IEEE Transactions on Energy Conversion* 1994; **9**(4):652–658.
3. Thomson WT, Fenger M. Current signature analysis to detect induction motor faults. *IEEE Industry Applications Magazine* 2001; **7**(4):26–34.
4. Bellini A, Filippetti F, Franceschini G, Tassoni C, Kliman GB. Quantitative evaluation of induction motor broken bars by means of electrical signature analysis. *IEEE Transactions on Industry Applications* 2001; **37**(5):1248–1255.
5. Milimonfared J, Kelk HM, Nandi S. A novel approach for broken rotor bar detection in cage induction motors. *IEEE Transactions on Industry Applications* 1999; **35**(5):1000–1006.
6. Nandi S, Toliyat HA. Condition monitoring and fault diagnosis of electrical machines—a review. *Proceedings of the IAS Annual Meeting (IAS'99)*, Vol. 1, 1999; pp 197–204.
7. Anderson P. *Analysis of Faulted Power Systems*. Iowa University Press, 1973.
8. Kezunovic M, Soljanin E, Perunicic B, Levi S. New approach to the design of digital algorithms for electric power measurements. *IEEE Transactions on Power Delivery* 1991; **6**(2):516–523.
9. Kezunovic M, Perunicic B. Digital signal processing algorithms for power quality assessment. *Proceedings of IEEE–IECON'92*, San Diego, California, U.S.A., November 1992; pp 1370–1375.
10. Begovic MM, Djuric PM, Dunlap S, Phadke AG. Frequency tracking in power networks in the presence of harmonics. *IEEE Transactions on Power Delivery* 1993; **8**(2):480–486.
11. Smith SW. *The Scientist and Engineer's Guide to Digital Signal Processing*. California Technical Publishing, 1997.
12. Oppenheim AV, Schafer RW, Buck JR. *Discrete Time Signal Processing*. Prentice Hall, 1999.
13. Lobos T. Fast estimation of symmetrical components in real time. *IEE Proceedings—C* 1992; **139**(1): 27–30.
14. Campos A, Joos G, Ziogas PD, Findlay JF. A DSP-based real-time digital filter for symmetrical components. *Proceedings of the Athens Power Technology Conference*, Vol. 1, Athens, Greece, September 1993; pp 75–79.
15. Soliman SA, Mostafa MA, El-Hawary MA, Al-Kandari AM. Two digital filtering algorithms for fast estimation of symmetrical components in a power system: a static estimation approach. *Proceedings of the Large Engineering System Conference on Power Engineering LESCOPE'01*, 2001; pp 125–130.
16. Sottile J, Kohler JL. An on-line method to detect incipient failure of turn insulation in random-wound motors. *IEEE Transactions on Energy Conversion* 1993; **8**(4):762–768.
17. Henao H, Capolino GA, Assaf T, Cabanas MF, Melero MG, Orcajo GA, Cano JM, Briz del Blanco F. A new mathematical procedure for the computation of the inverse sequence impedance in working induction motors. *Proceedings of the IAS Annual Meeting (IAS'00)*, Vol. 1, Rome, Italy, October 2000; pp 336–343.
18. Assaf T, Henao H, Capolino GA. Detection of voltage source dissymmetry using the measurement of the symmetrical components in working induction motors. *Proceedings of IEEE-SDEMPED'01*, Gorizia, Italy, September 2001.
19. Assaf T. A spectral method for the computation of symmetrical components for induction machines (in French). *National Meeting of Graduate Students on Electrical Power Engineering, JCGE'01*, Nancy, France, November 2001; pp 141–146.

AUTHORS' BIOGRAPHIES

T. Assaf received the M.S. degree in electrical engineering from the University of Sciences and Techniques of Lille in 1999. Since then, he has been preparing his Ph.D. at the Department of Electrical Engineering of the University of Picardie 'Jules Verne', Amiens, under the supervision of Professor G.A. Capolino and Dr H. Henao. He has received grants from the Syrian Government. His research interests are electrical machines and drives for which he has developed methods to detect electrical faults using voltage, current and flux sensors.

H. Henao received the M.S. degree in electrical engineering from Universidad Tecnologica de Pereira, Colombia in 1983, the M.S. degree in power system planning from Universidad de los Andes, Bogota, Colombia, in 1986, and the Ph.D degree in electrical engineering from Institut National Polytechnique de Grenoble in 1990.

From 1987 to 1994, he was a consultant for Schneider Industries and GEC Alsthom in the Modeling and Control Systems Laboratory, Mediterranean Institute of Technology, Marseille. In 1994, he joined the Ecole Supérieure d'Ingénieurs en Electrotechnique et Electronique, Amiens, as Associate Professor. In 1995, he joined the University of Picardie 'Jules Verne' as an Associate Professor in the Department of Electrical Engineering. He is currently the Department representative for the international programs and exchanges (SOCRATES).

Dr Henao's main research interests are the modelling, simulation monitoring and diagnosis of electrical machines and electrical drives.

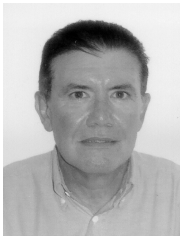

G. A. Capolino received the B.S. degree in electrical engineering from Ecole Supérieure d'Ingénieurs de Marseille in 1974, the M.S. degree in electrical engineering from Ecole Supérieure d'Electricité, Paris, in 1975, the Ph.D. degree in electrical engineering and computer science from University Aix-Marseille I in 1978 and the D.Sc. degree in engineering sciences from Institut National Polytechnique de Grenoble in 1987.

In 1978, he joined the University of Yaoundé, Cameroon, as an Associate Professor and Head of the Department of Electrical Engineering. From 1981 to 1994, he was Associate Professor at the University of Dijon and the Mediterranean Institute of Technology, Marseille, where he was founder and Director of the Modelling and Control Systems Laboratory. From 1983 to 1985, he was visiting Professor at University of Tunis, Tunisia. From 1987 to 1989, he was the scientific advisor of Technicatome SA in the field of electrical drives for nuclear propulsion. In 1994, he joined the University of Picardie 'Jules Verne' as a Full Professor, as Head of the Department of Electrical Engineering from 1995 to 1998 and Director of the Energy Conversion and Intelligent Systems Laboratory from 1995 to 1999. He is currently the Director of Graduate Studies in electrical engineering for the University of Picardie 'Jules Verne'.

Professor Capolino's research interests are electrical machines, power electronics and electrical drives for which he has introduced new techniques of modelling, control and simulation. He has developed new courses in power electrical engineering based on computer assistance. He has published more than 200 papers in scientific journals and conference proceedings and has co-authored the book *Simulation & CAD for Electrical Machines, Power Electronics and Drives* (ERASMUS Program Edition, Brussels, 1991).

Professor Capolino is a Fellow of the IEEE and is currently an Associate Editor of the *IEEE Transactions on Industrial Electronics*.